

Path Planning of 6-DOF Venipuncture Robot Arm Based on Improved A-star and Collision Detection Algorithms

Fenglei Li^{1, 2}, Zexin Huang^{1, 2}, and Lin Xu^{1, 2 *}

1. Institute of Robotics and Automatic Information Systems, Nankai University, Haihe Education Park, Tianjin 300350, China
2. Tianjin Key Laboratory of Intelligent Robotics, Nankai University, Haihe Education Park, Tianjin 300350, China

Abstract—In this paper, we use a compact 6 degree-of-freedom (DOF) robot arm as the actuator of the venipuncture system. Aiming at the robot arm's requirements for speed and smoothness and considering that the robot arm may collide with obstacles in the course of movement, we simplify the model of the robot arm and obstacles according to the geometry of the robot arm and obstacles in the environment. Then we proposed an improved A-star algorithm and a three-dimensional (3D) collision detection algorithm, which can plan a collision-free optimal path for the blood taking needle fixed in the end of the robot arm, so that the blood taking needle can penetrate into the target point of the venous vessel continuously, smoothly and accurately driven by the robot arm. The simulation and actual path planning experiments indicate that the proposed path planning method is effective and feasible.

Index Terms-Robot arm, Venipuncture, planning, Improved A-Star algorithm, Collision detection algorithm

I. INTRODUCTION

The automated venipuncture robot is a device specially used to replace nurses to perform venipuncture on patients. It can automatically locate the 3D position of the venous blood vessel and complete the needle insertion and withdrawal. The operation procedure and time are similar to those of human nurses. This can effectively reduce the labor costs of hospitals and improve the level of medical services. In recent years, several prototypes of automatic venipuncture robotic system are proposed. In 2013, T.S.Perry developed a venipuncture robot based on ultrasound and stereovision. It used a 6-DOF industrial manipulator as the puncture actuator, and carried out path planning and actual puncture experiments on the puncture mechanism [1]. It is said that the success rate of puncture was 83%. In 2015, Max L.Balter et al. developed a venipuncture robot based on stereovision, ultrasound and force guidance [2]. Its puncture actuator is a compact 7-DOF manipulator, and a simple needle path planning is carried out. In 2017, Zixing Li et al. developed a prototype of a 5-DOF venipuncture robot, and studied the force of the blood taking needle [3]. The venipuncture needle is driven by a linear guide that moves over the blood vessel and inserts into the blood vessel with three translational DOF.

However, above three venipuncture robot prototype systems only performed simple path planning for the needle, and did not take into account factors such as shortest path and collision detection, which may cause some troubles. In

This work is supported by the Fundamental Research Funds for the Central Universities and the National Natural Science Foundation of China(NSFC Grant No.61873135).

* Corresponding author, email: xul@nankai.edu.cn.

the prototype of the venipuncture robotic system developed by our team, we chose a compact 6-DOF robot arm as the executing mechanism of the puncture task. It is a portable robot arm, easy to control and has a large working pose range. The needle is attached to end of the robot arm and is driven to complete the venipuncture task. In our system, due to the existence of many obstacles, collision detection processing is also performed while planning a short smooth path at a rapid planning. How to quickly plan an optimal collision-free path for the needle while performing collision detection, so that the blood taking needle can complete the puncture task quickly and accurately while the system is working, which is a challenge we will face.

After the target point of puncture is determined, path planning becomes the key step for the venipuncture robot. The path planning of the robot arm is to find an optimal or better collision-free path from the initial state to the target state in the workspace [4]. In order to enable the robot arm to perform the venipuncture task quickly and accurately, we not only ensure the robot arm smoothly moves to the target along the path, but also ensure the robot arm cannot collide during the movement.

In the field of path planning for robotic arm, many researchers proposed different path planning methods according to specific application scenarios and verified them in recent years. Wang Shou-kun proposed a method to plan path for 6-DOF manipulator based on navigation potential function [4], which can solve the problem of local minima in traditional potential method. Palitha Dassanayake et.al proposed a motion planning method for robots based on fuzzy behavior[5]. Han Tao et al. proposed a real-time path planning method for manipulator based on genetic algorithm [6]. Chao Ma proposed an approach for 6R serial manipulator path planning by using RRT algorithm [7], and proved the feasible and effective of this method after carrying out simulation experiments. X.J.WU et.al s proposed a practical on-line robot motion planning approach to search collision-free path in the configuration space by using A* algorithm and achieved good results[8]. Ao Jiang proposed an obstacle avoidance path planning algorithm based on genetic algorithm for the problem that the manipulator might collide with obstacles in the workspace [9]. Y. Kim et al. present a path planning algorithm with RRT for a 7 DOF manipulator and verifying this method by a numerical simulation [10]. However, these methods have complex modeling or computational complexity. In order to meet the requirements of needle

puncture in our automatic venipuncture system for speed and smoothness, we proposed an improved A* algorithm combined with a 3D collision detection algorithm to plan a suitable and smooth collision-free path in the Cartesian space for the 6-DOF robot arm.

This paper is organized as follows. Section II introduces the D-H parameters and kinematics analysis of the robot arm. Section III describes the 3D obstacle modelling, collision detection and improved A* algorithm. Section IV designs experiments to evaluate our proposed path planning algorithm. Section V concludes the paper.

II. KINEMATICS ANALYSIS OF THE ROBOT ARM

A. Structure of the venipuncture robot

The prototype of the venipuncture robot system developed by our research group is shown in Fig. It mainly consists of two parts. The first part is the image acquisition and processing part, and the second part is the 6-DOF robot arm used for needle puncture.

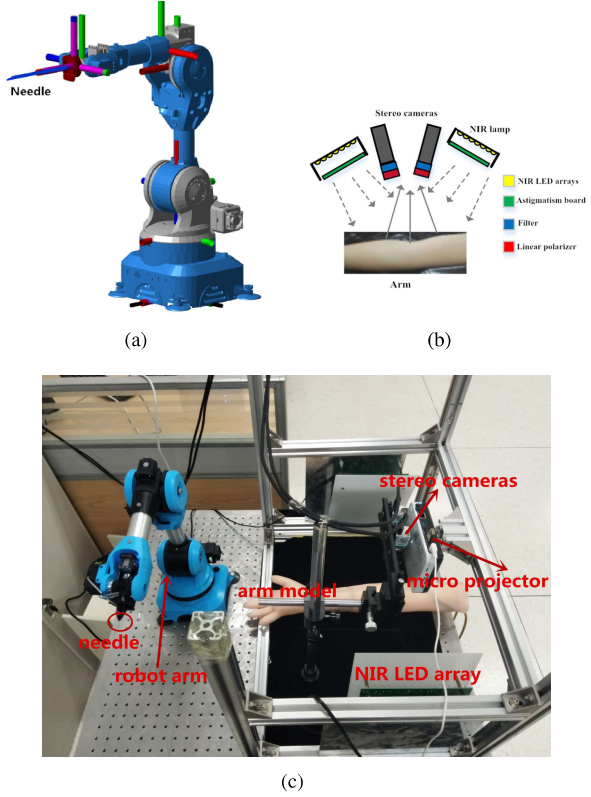


Fig. 1. (a) Venous puncture robot arm schematic. (b) Image acquisition and processing part schematic diagram. (c) Prototype of the venipuncture robotic system.

1) Image Acquisition and Processing: This part is to obtain 3D information of the subcutaneous venous blood vessels, and select the appropriate venipuncture target point. Firstly, we obtain 3D model of the arm skin surface based on binocular structured light reconstruction method [11]. Secondly, we obtain 3D model of the subcutaneous venous blood vessel based on near-infrared light stereo reconstruction method. Then, the arm surface model and venous blood

vessel model are fused by means of binocular camera multiplexing. And the complete 3D model of the subcutaneous venous blood is obtained. Finally, based on the radius, curvature, depth and other indicators of the blood vessel, an appropriate vascular puncture target point is selected for the blood taking needle. The schematic diagram of image acquisition and processing is shown in Fig.2.

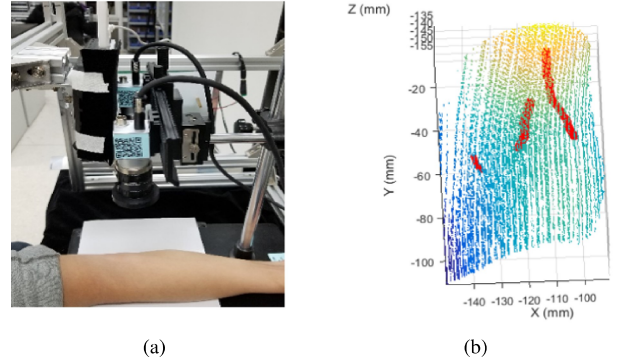


Fig. 2. (a) Prototype of the image acquisition and processing part.(b) 3D point cloud image of the venous blood vessels after model fusion.

2) The puncture robot arm: The second part of the venipuncture robot is mainly researched in this paper. The robot arm studied in this paper is a 6-DOF desktop robot arm, which has 6 rotating joints [12], as shown in Fig.3(a).The coordinate system of each link is established according to the actual connection of the robot arm by using the Denavit-Hartenberg method [13], as shown in Fig.3(b).

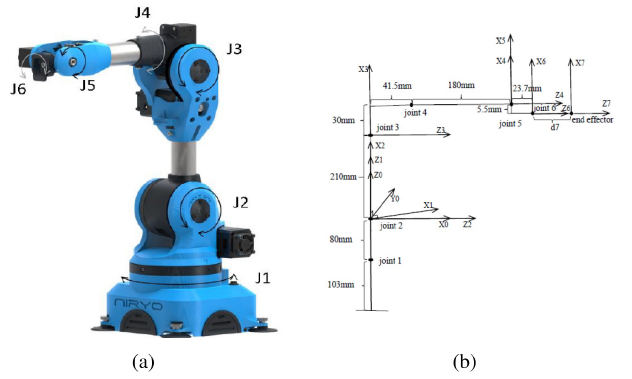


Fig. 3. (a) The directions of its joints rotation [12]. (b) Coordinate axes and mechanical dimensions of the robot arm.

According to the established link coordinate system, we can get the D-H parameter table listed in Table I.

B. Forward Kinematic of the robot arm

Then, we can perform kinematic analysis on the robot arm. According to the above D-H parameter table, the homogeneous transformation matrix between the end-effector's coordinate system and the robot arm's base coordinate system can be derived as equation(1).

$${}^0_{\text{endEffector}} \mathbf{T} = {}^0_1 \mathbf{T}(\theta_1) * {}^1_2 \mathbf{T}(\theta_2) * \dots * {}^6_{\text{endEffector}} \mathbf{T}(\theta_7) \quad (1)$$

TABLE I
D-H PARAMETERS OF THE ROBOT ARM

Link i	$\alpha_{i-1}/^\circ$	a_{i-1}/m	d_i/m	θ_i	Joints range/°
1	0	0	0	θ_1	(-175,175)
2	90	0	0	θ_2	(-90,36.7)
3	0	0.21	0	θ_3	(-80,90)
4	90	0.03	0.2215	θ_4	(-175,175)
5	-90	0	0	θ_5	(-100,110)
6	90	-0.0055	0.0237	θ_6	(-147.5,147.5)

C. Inverse Kinematics of the robot arm

Generally, the inverse solution method of the robot arm can be divided into two categories: closed-form solutions and numerical solutions. The condition that the robot arm can find closed-form solutions is to meets the Pieper criterion [14]. That is, a sufficient condition for the manipulator with six rotating joints to have a closed solution is that the adjacent three joint axes intersect at one point. From the link coordinate system established above, since the mechanical structure of the robot arm we use does not conform to the Pieper criterion, so we can't get a closed-form solutions. In this paper, we use the Inverse Kinematics function in MATLAB to find the inverse kinematics solution of the robot arm which is convenient.

III. COLLISION DETECTION ALGORITHM

A. Obstacles Modeling

Obstacles in 3D space generally have irregular geometric shapes, so it is not easy to model accurately. In order to facilitate the calculation and improve the efficiency of collision detection, we use the bounding box method [15] to simplify the obstacles in the body and the environment, and replace them with different regular geometry in this paper. In this paper, we use some envelopes to simplify the obstacles in the environment, and use those envelopes as obstacle model information in the environment such as cuboid, cylinder and sphere.

B. Robotic Arm Simplification

The robot arm is a chain structure composed of a plurality of joints. In this paper we use the cylindrical envelope method to simplify the joints and end effectors of the robot arm with 5 cylinder envelopes. The cylindrical envelope method is to surround each link of the robot arm with a cylinder of a certain radius. These cylinders are just enough to completely enclose the connecting rod.

C. Collision Detection

In the process of the multi-joints robot arm obstacle-free path planning, the obstacle avoidance problem of the robot arm mainly includes two aspects: one is the collision between the joints of the robot arm, and the other is collision of the robot arm with obstacles in the working space.

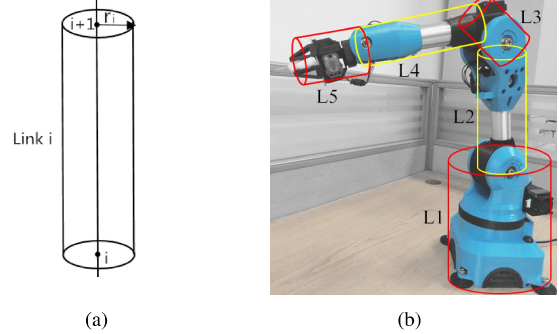


Fig. 4. (a) Simplifying the link with a cylinder envelope of radius. (b) Simplifying the manipulator with five cylinder envelopes.

1) *Self-collision detection of the robot arm:* After simplifying the manipulator with five cylindrical envelopes, we can perform self-collision detection of the robot arm. For the collision problem of two links, we can translate into the problem of whether the two cylinder envelopes in the space intersect. A schematic diagram of the intersection of two cylinder envelopes is shown in Fig.5 below.

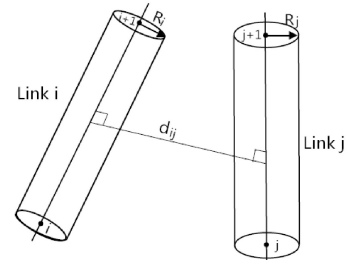


Fig. 5. Positional relationship of two cylinders.

2) *External collision detection of the robot arm:* We simplified the robot arm with a cylindrical box and enveloped the obstacles in the space with rectangular boxes. Then we can transform the collision detection problem of the arm body and the obstacles in the environment into the positional relationship problem between the cylinder and the cuboid in space. In this paper, we superimpose the radius of the cylinder envelope on the cuboid envelope of the obstacle to form a new cuboid envelope. Then we can detect the collision by calculating whether the center line segment of link and the six faces of have intersections. The process is shown in Fig.6.

Similarly, the collision detection between the robot arm and the cylindrical envelope obstacle is equivalent to the judgment of the position relationship between the two cylinders in space.

IV. IMPROVED A-STAR ALGORITHM

A. Standard A-star algorithm

The A-star (A^*) algorithm is a heuristic search algorithm. It can be used to search for an optimal path from the initial node to the target node in the workspace.

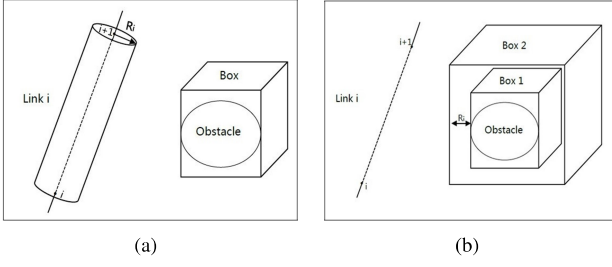


Fig. 6. (a) Positional relationship between cylinder envelope and cuboid envelope. (b) Line segment and the extended cuboid.

A* algorithm uses an evaluation function $f(n)$ to guide the selection of best node in the current nodes. Its core idea is to select the node with the lowest $f(n)$ value in the nodes to be selected.

Assume that the initial node is $(x_{start}, y_{start}, z_{start})$, the target node is $(x_{goal}, y_{goal}, z_{goal})$, the currently selected node is (x_n, y_n, z_n) . Then the evaluation function $f(n)$ can be described as equation (2).

$$f(n) = g(n) + h(n) \quad (2)$$

Where function $g(n)$ represents the actual path cost from the initial node to the current node.

$$g(n) = \sum_{i=2}^{i=n} \sqrt{(x_i - x_{i-1})^2 + (y_i - y_{i-1})^2 + (z_i - z_{i-1})^2} \quad (3)$$

The function $h(n)$ represents the evaluation cost from current node to target node. Euclidean distance and Manhattan distance are commonly used evaluation criteria for $h(n)$. This paper uses Manhattan distance to evaluate $h(n)$.

$$h(n) = |x_n - x_{goal}| + |y_n - y_{goal}| + |z_n - z_{goal}| \quad (4)$$

B. Improved A-star algorithm

There is an obvious disadvantage in applying A* algorithm to the 3D path planning of manipulator: when the search space of A* algorithm increases or the search step size decreases, the calculation amount of A* algorithm increases exponentially, which makes the time of path search very long. Aiming at the shortcomings of A* algorithm in searching path in 3D space, we propose an improved A* algorithm for path planning of multi-DOF robot arm. We propose three improvements based on the original A* algorithm.

1) First: Aiming at the application environment of the venipuncture robot, we use A* algorithm to plan the path in Cartesian space, and make the position and pose of blood taking needle on the end of the robot arm change evenly between the adjacent path points of the path planning. The step size in length is set to be $stepSize$. The variation of the posture of blood taking needle between adjacent waypoints (expressed by RPY angle) are showed below, and N is the number of path segments.

$$\begin{cases} \Delta R = (R_{goal} - R_{initial})/N \\ \Delta P = (P_{goal} - P_{initial})/N \\ \Delta Y = (Y_{goal} - Y_{initial})/N \end{cases} \quad (5)$$

2) Second: We use the Manhattan distance as the criterion for evaluating the function $h(n)$. The lowest evaluation value $f(n)$ is selected among all the adjacent path points of the current path point. If the lowest evaluation value $f(n)$ has more than one path points, then we select the waypoint closest to the starting-ending line. In this way, we can ensure that the improved A* algorithm can complete the path planning at fast speed and avoid unnecessary calculation. Fig.7 is the schematic diagram.

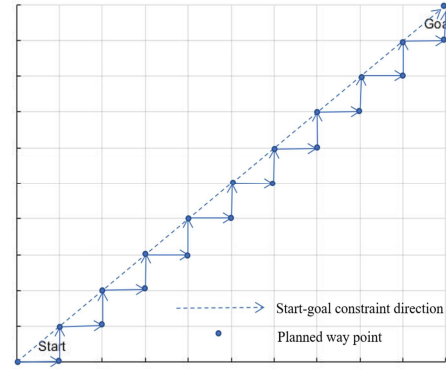


Fig. 7. starting-ending line direction constraint diagram.

3) Third: Delete the redundant points of the path points to make the path shorter and smoother. The specific steps are as follows: starting from the first path point, every three path points are grouped. When the connection line between the first path point and the third path point in each group does not collide with the obstacles in the environment, the second path point of the group which extend path length will be removed, and then the next detection is carried out. Finally, the planned path is shorter and the number of bends is less.

V. EXPERIMENT AND ANALYSIS

A. Path planning and experiment verification

In this paper, the process of blood taking needle path planning is shown in Fig.8. In our venipuncture robot system, the system first obtains the 3D information of the subcutaneous vein by stereoscopic imaging, and selects the appropriate puncture target point according to the 3D information of the blood vessel. We then use the stereo calibration and hand-eye calibration to convert the pose of needle at the puncture target point into the pose in the robot arm base coordinate. The initial position and posture of the robot arm in the venipuncture robot system are known. The position of the blood taking needle at the starting point is $P_{initial} = [0.2922m, 0m, 0.4175m]$, and its rotating Euler angle is $RPY_{initial} = [0rad, 0rad, 0rad]$.

So the homogeneous transformation matrix of the blood taking needle in the initial state is follows.

$$T_{initial} = \begin{bmatrix} 1 & 0 & 0 & 0.2922 \\ 0 & 1 & 0 & 0.0000 \\ 0 & 0 & 1 & 0.4175 \\ 0 & 0 & 0 & 1.0000 \end{bmatrix} \quad (6)$$

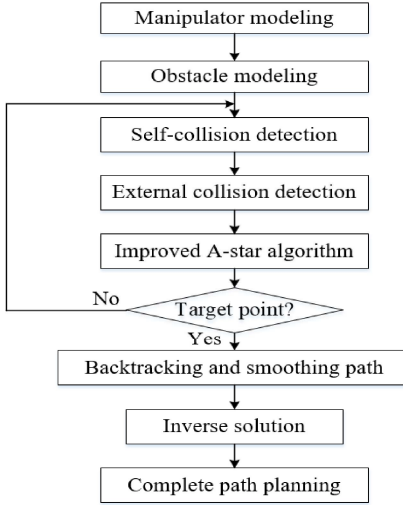


Fig. 8. Process of blood taking needle path planning.

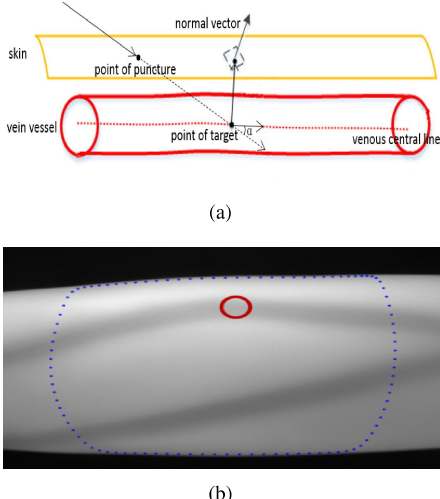


Fig. 9. (a) Schematic diagram of selected skin puncture points and vascular target points. (b) Selected vessel target point (red circle).

After image acquisition and processing, we selected the target point of needle. The schematic diagram of selected puncture point is shown as Fig.9. Assuming that when the needle tip reaches the target point of blood vessel, the angle α between the needle tip and the central line of blood vessel is 30° . Finally, after the process of stereo cameras calibration and hand-eye calibration, we get the pose of needle at the target point (in the robot arm's coordinate system) as follows.

$$T_{goal} = \begin{bmatrix} -0.1558 & -0.9561 & 0.2408 & -0.0068 \\ 0.9117 & -0.0467 & 0.4037 & 0.5428 \\ -0.3766 & 0.2825 & 0.8821 & 0.1557 \\ 0 & 0 & 0 & 1.0000 \end{bmatrix} \quad (7)$$

Then the position of the needle in the target point is $P_{goal} = [-0.0068m, 0.5428m, 0.1557m]$. And the needle's rotation Euler angle is $RPY_{goal} = [0.3099rad, 0.3862rad, 1.7401rad]$. In this paper, the

search space range is set to $1.0m * 1.0m * 0.8m$ according to the workspace of the robot arm, the search space range is divided by cubes of the same size, and $stepSize$ is set to $0.05m$.

The path planning is performed on MATLAB2018b, and the platform is Dell XPS 8930 desktop computer with Intel Core i7-8500 CPU. We use the improved A* algorithm and collision detection algorithm proposed in this paper to plan a collision-free path for the blood collection needle. We obtain the angular sequence value of the robot arm by inverse kinematics on the path poses after smoothing the path. The initial state and modeling of the robot arm are shown in Fig.10. The final results are shown in Fig.11.

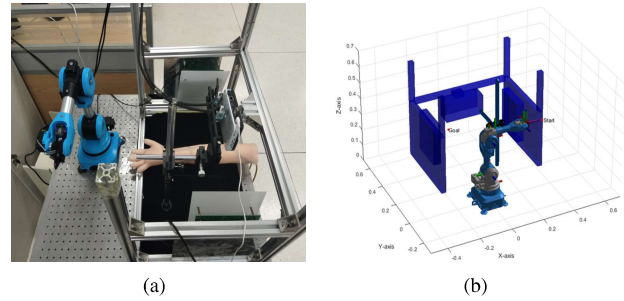


Fig. 10. (a) Initial state of the robot arm and (b) corresponding simulation modeling.

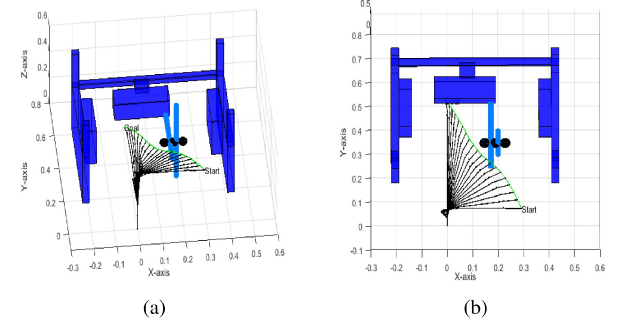


Fig. 11. Needle planning path after 3-point smoothing and corresponding robot arm configuration. (a) Front view.(b) Top view.

B. Comparison experiments

In order to verify the validity and optimality of the path planning algorithm used in this paper, we use Rapidly Exploring Random Tree(RRT) algorithm, Artificial Potential Field (APF) algorithm and A* algorithm to plan a collision-free path for the needle respectively as comparative experiments. These comparative experiments are carried out under the same conditions. The obstacle setting and destination pose of the comparative experiments are exactly the same as the path planning experiment based on the improved A-star algorithm in the previous section. Table II is the comparative experiments results.

From Table II, we can see that the improved A* algorithm proposed in this paper has the advantages of shorter path

TABLE II
COMPARISON OF EXPERIMENTS RESULTS

Algorithm	PathLength/m	time/s	Smoothness
RRT	0.9794	190.7504	<i>Rough</i>
APF	0.8515	202.4781	<i>Relatively smooth</i>
A*	0.7026	1842.8324	<i>Relatively smooth</i>
Improved A*	0.6548	5.7629	<i>Smoothest</i>

and shorter search time than the other three path planning algorithms. It is common that the smoother the needle puncture path is, the less resistance the needle receives from the skin tissue. This can improve the success rate of venipuncture and reduce the pain of patients. In those comparison experiments in this section, the path planned using improved A-star algorithm is the smoothest, which can meet the path smoothness requirement of venipuncture.

C. Actual venipuncture experiment

In this section, we perform actual venipuncture experiment on the robot arm with the planned path. The joint angle sequence values corresponding to the planned path points in is input into the 6-DOF robot arm through instructions, and the robot arm is controlled to drive the blood taking needle along the planned path to complete the venipuncture task. The experimental results are shown in Fig. 12.

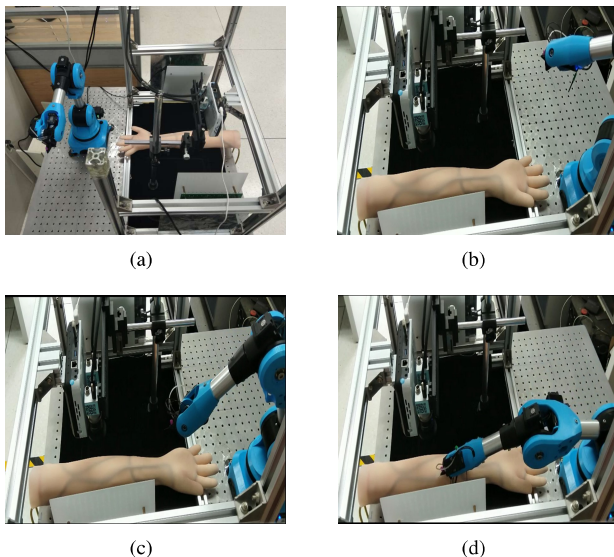


Fig. 12. The actual movement of robot arm in experiment. (a) is initial configuration of the robot arm, (b)-(c) are two configurations in the movement,(d) is end configuration of the robot arm.

In the actual venipuncture experiment, the needle fixed on end effector of the robot arm is successfully inserted into the target point of the blood vessel, which demonstrates the effectiveness and feasibility of the path planning algorithm proposed in this paper.

VI. CONCLUSION

In this paper, we presented an approach for autonomous path planning of the 6-DOF robot arm for venipuncture requirements based on collision detection and improved A* algorithm. The results of simulation experiment and actual venipuncture experiment demonstrate that our proposed method can better solve the plan planning problem of the 6-DOF robot arm. By comparing this method with the path planning algorithm for multi-DOF robot arm based on RRT algorithm, Artificial Potential Field algorithm and standard A* algorithm respectively, we can prove that our proposed path planning method is feasibility and optimal between those algorithms. And our proposed algorithm can meet the puncture robot arm's requirements for speed and path smoothness.

REFERENCES

- [1] T.S.Perry, "Profile veebot-Drawing blood faster and more safely than a human can," IEEE Spectrum. Vol.50,no.8,pp.23-23,Aug.2013.
- [2] M. Balter, A. Chen, T. Maguire, and M. Yarmush, "The system design and evaluation of a 7-DOF image-guided venipuncture robot,"IEEE Trans. Robot., vol. 31, no. 4, pp. 1044-1053, Aug. 2015.
- [3] Zixing Li, Mingwei Li, "A robotic system for investigation on mis-alignment force of needle and vein needle insertion into blood vessel,"2017 2nd Asia-Pacific Conference on Intelligent Robot Systems (ACIRS), 2017: 280 - 283.
- [4] WANG Shou-kun,Zhu Lei,WANG Jun-zheng,"Path Plan of 6-DOF Robot Manipulators in Obstacle Environment Based on Navigation Potential Function," transactions of Beijing Institute of Technology, 2015,35(02),pp186-191.
- [5] P.Dassanayake,K.Watanabe,"Fuzzy Behavior-Based Motion Planning for the PUMA Robot",Proceedings of the 2000 IEEE/RSJ International Conference on Intelligent Robots and Systems,pp.1912-1916,2000.
- [6] Tao Han, Huaiyu Wu,"Research on path planning for manipulator to avoid real-time obstacle based on genetic algorithms," Application Research of Computers, Vol.30 No.5, ,1373-1376,May.2013.
- [7] C. Ma, Y. Zhang, Q. Zhao and K. Bai, "6R Serial Manipulator Space Path Planning Based on RRT," 2016 8th International Conference on Intelligent Human-Machine Systems and Cybernetics (IHMSC), Hangzhou, 2016, pp. 99-102.
- [8] X.J.Wu, J.Tang, "Development of a configuration space motion planner for robot in dynamic environment," Robotics and Computer Integrated Manufacturing, 2009,25:13-31.
- [9] Ao Jiang,Xiang Yao,Juan Zhou,"Research on path planning of real-time obstacle avoidance of mechanical arm based on genetic algorithm",The 2nd 2018 Asia Conference on Artificial Intelligence Technology,pp.1579-1586,2018.
- [10] Y. Kim, J. Wang, S. Park, J. Lee, J. Kim and J. Lee, "A RRT-based collision-free and occlusion-free path planning method for a 7DOF manipulator," 2014 IEEE International Conference on Mechatronics and Automation, Tianjin, 2014, pp. 1017-1021.
- [11] T.P.Koninckx, L.Van Gool,"Real-time range acquisition by adaptive structured light," IEEE Transactions on Pattern Analysis and Machine Intelligence,2006,28(3):432-445.
- [12] [Online],"Niryo One Mechanica Specifications,https://niryo.com/."
- [13] J.Denavit and R.S.Hartenberg,"A Kinematic Notation for Low-Pair Mechanisms Based on Matrices,"Journal of Applied Mechanics,pp.215-221,June 1955.
- [14] D.Pieper and B.Roth,"The Kinematics of Manipulators Under Computer Control,"Proceeding of the Second International Congress on Theory of Machines and Mechanisms, Vol.2,Zakopane,Poland,1969,pp.159-169.
- [15] Bao WeiWei,"Reserch on Multi-joint Repairing Manipulator's Obstacle Avoidance Path Planning," Harbin Engineering University, March,2009.
- [16] CAI Di,XIE Cun-xi,"Study on workspace analysis and simulation of 6-DOF painting robot based on monte-carlo method," Machinery Design and Manufacture, No.3,pp.161-162,Mar.2009.